

# A Simple Empirical Equation to Calculate Cloud Optical Thickness from Shortwave Broadband Measurements

*J. C. Barnard and C. N. Long  
Pacific Northwest National Laboratory  
Richland, Washington*

## Introduction

Observational studies of shortwave cloud optical thickness,  $\tau_c$ , play an important role in determining how clouds affect climate. Accordingly, considerable effort has been, and continues to be expended to characterize the spatial and temporal distribution of  $\tau_c$  over the globe. This effort involves satellite and ground-based measurements that infer  $\tau_c$  from measurements of the reflection or transmission of solar radiation. Transmitted solar radiation forms the basis of several important algorithms designed to calculate  $\tau_c$ ; these algorithms use either spectral irradiances (Min and Harrison 1996; henceforth referred to as the “Min algorithm”) or broadband irradiances (Dong et al. 1997; Boers 1997; Barnard et al. 2001). The Min algorithm runs relatively quickly on a desktop personal computer, but requires spectral irradiance at one wavelength. This information is often not readily available, thus limiting the opportunity of using the Min algorithm at a wide variety of sites.

On the other hand, shortwave broadband irradiances are commonly measured, but the algorithms that use these measurements are computationally very slow. This makes the algorithms impractical for routine calculations of cloud optical thickness over many sites and over long periods of time. With this limitation in mind, it is desirable to find another method of calculating cloud optical thickness that is computationally quick, while retaining the flexibility to use broadband shortwave irradiances as input. To this end, we have developed a simple empirical relationship that links broadband irradiances to cloud optical thickness.

## Procedure

The goal of our empirical approach is to find some approximate functional relationship between the solar broadband irradiances and cloud optical thickness,

$$\tau_c^e = f(r) \quad (1)$$

where  $r$ , to be determined, is some dimensionless combination of broadband irradiances and the cosine of the solar zenith angle,  $\mu_0$ ; and  $\tau_c^e$  is the estimated cloud optical thickness (explicitly denoted by the superscript “e”). To establish this relationship, we must determine both the variable  $r$  and the function  $f$ . This is a trial and error process consisting of several steps, described as follows. First, using various

combinations of  $\mu_0$ , the broadband irradiances, or quantities derived from them, we define a tentative  $r$ . For each time that a value of  $r$  is calculated, the Min algorithm is used to determine the cloud optical thickness; we denote this as  $\tau_c^M$  (distinguished from  $\tau_c^e$  by the superscript “M”). We accept  $\tau_c^M$  as truth, and by plotting  $\tau_c^M$  versus  $r$  for a wide range of  $r$ , we hope to find a particular form for  $r$  such that the  $\tau_c^M$  collapse on a single curve. This collapse implies that a one-to-one relationship exists between  $r$  and  $\tau_c^M$ —an obviously desirable situation. In practice, a perfect collapse is rarely achieved so we must content ourselves with “near” collapse, which we assess visually by examining plots constructed using different forms for  $r$ .

This trial and error approach was followed using various  $r$ 's until we found one that provided the hoped-for (near) collapse. The final  $r$  that we settled on is defined as

$$r = \frac{D}{C\mu_0^{1/4}} \quad (2)$$

where  $D$  is the measured diffuse irradiance, corrected using the Dutton method (Dutton et al. 2001), and  $C$  is the total, downwelling “clear-sky” irradiance from the analysis of Long (2001) and Long and Ackerman (2000).

This trial and error process requires collocated spectral and broadband irradiances. The spectral data required by the Min algorithm is obtained from the multifilter rotating shadowband radiometer (MFRSR), while  $r$  is determined from broadband radiometers that measure the diffuse, total, and direct components of the shortwave irradiance. These data come from a geographically diverse set of sites in the Atmospheric Radiation Measurement (ARM) system: two facilities, E13 and E22, located at ARM's Southern Great Plains (SGP) site, the Barrow facility from the North Slope of Alaska (NSA) site, and the Manus facility from the ARM's Tropical Western Pacific (TWP) observational network. For each geographical region, there are about 8000 points representing 5-minute averages of cloud optical thickness over the year 2000. Figure 1 shows the  $\log[\tau_c^M]$  plotted versus the value of  $r$  defined in Eq. 2. The cloud optical thicknesses from each site have been color coded, so that the blue, red, and green symbols represent  $\tau_c^M$  from the NSA, TWP, and SGP sites, respectively.

Figure 1 does indeed reveal a near collapse of the data, and encouragingly, this collapse is consistent from one geographical site to another. The solid back line in this figure shows a function,  $f$ , fit to these data. This function is assumed to have the form of a hyperbolic arctangent

$$\tau_c^e = \text{Exp}[a + b \cdot \text{ArcTanh}(1 + c \cdot r)] \quad (3)$$

where  $a$ ,  $b$ , and  $c$  are the coefficients that are determined by using a least squares fitting routine to minimize the difference between  $\tau_c^M$  and  $\tau_c^e$ .

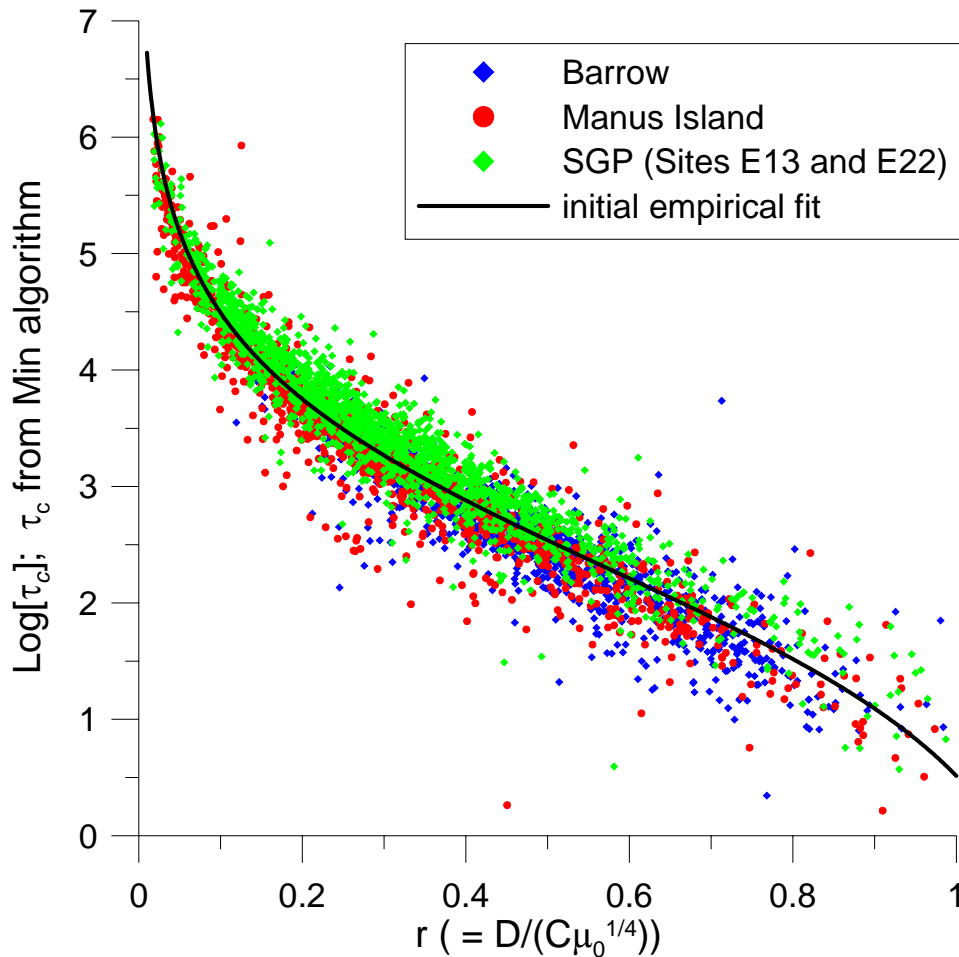


**Figure 1.** Log of cloud optical thickness, derived from the Min algorithm, plotted versus the variable,  $r$ . Data from three ARM sites are used in this plot as indicated by the color-coding. The black line in this figure shows a hyperbolic arc tangent fit to these data.

Equation 3 was then refined slightly after an analysis of computer simulations using the SBDART model (Ricchiuzzi et al. 1998). These simulations were designed to test the sensitivity of the empirical relationship, Eq. 3, to variations in surface pressure (a proxy for altitude), surface albedo, and cloud effective radius. For example, we ran the model for a given surface pressure, surface albedo, and effective radius for clear-sky and cloudy sky cases that encompassed a range of  $\mu_0$  extending from 0.15 to 0.95. For the clear-sky cases, we assumed an aerosol optical thickness of 0.10 at 550 nm, and these runs provided the variable,  $C$ , in Eq. 2. The cloudy cases were identical to the clear-sky cases, except a single layer of clouds with optical thickness ranging from 1 to 500 was included in these cases. From these cloudy simulations we obtained  $D$ . These two sets of simulations allowed the generation of plots similar to Figure 1. Indeed, for a “standard” case with a surface pressure equal to 1013 mb, an albedo of 0.15, and an effective radius of 8  $\mu\text{m}$ , the computer-generated points showed a collapse that was nearly identical to that shown in Figure 1.

We found that the empirical equation was not effected by changes in surface pressure and only minimally sensitive to changes in cloud droplet effective radius, over a plausible range of effective radii from 6  $\mu\text{m}$  to 14  $\mu\text{m}$ . The relationship was somewhat sensitive to variations in surface albedo, and using the simulations as a guide, we refined Eq. 3 to account for these variations. The refined, final equation (Eq. 4) is

$$\tau_c^e = \text{Exp}[2/15 + A + 1.91 \cdot \text{ArcTanh}(1 - 1.74 \cdot r)] \quad (4)$$

where A is the surface albedo (limited to a range from 0.0 to 0.3).

## Assessment of Method

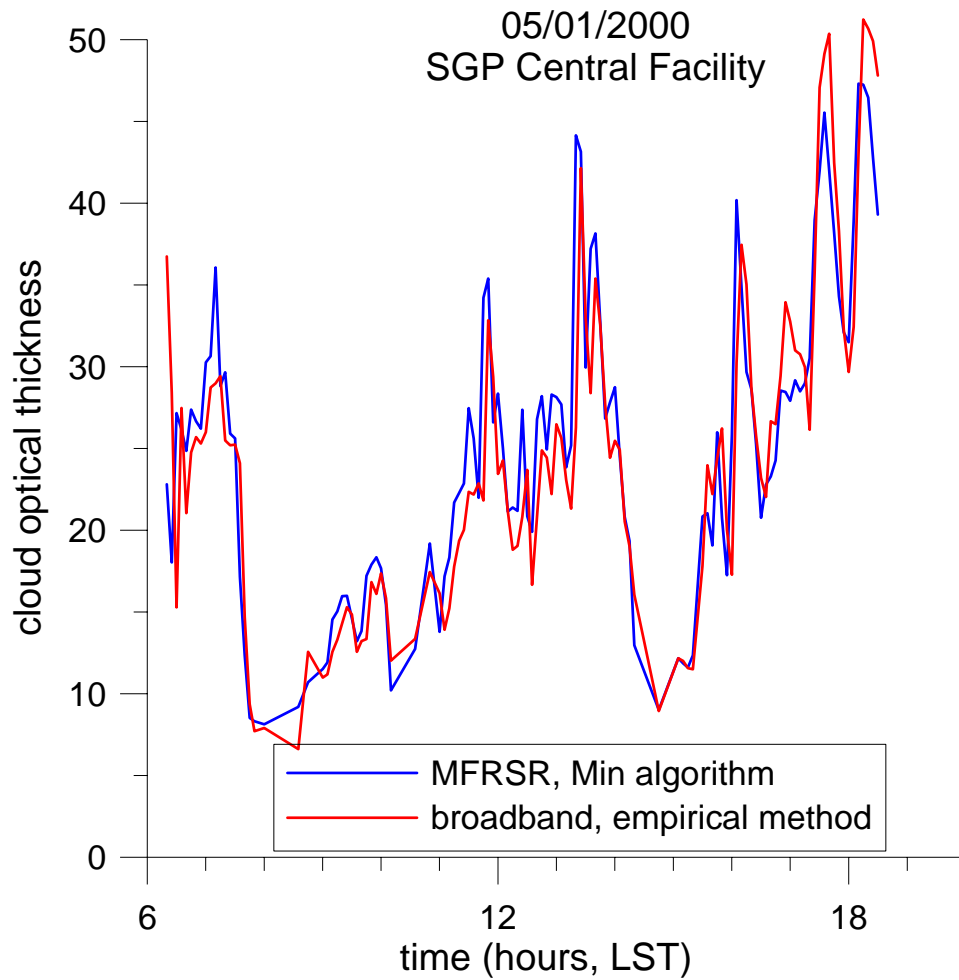
An important question regarding the use of Eq. 4 is: How well can it replicate our standard of truth, the optical thickness derived from the Min algorithm? The discrepancy between  $\tau_c^M$  and  $\tau_c^e$  can be examined in two ways: we can look, both visually and quantitatively, at the point-by-point error, defined as difference between of  $\tau_c^M - \tau_c^e$ , over a long period of time. Second, we can examine the error from a more global point of view, both visually and statistically, by comparing the distributions of  $\tau_c^M$  and  $\tau_c^e$ .

Figure 2 shows a visual assessment of the point-by-point error in which typical time series of both  $\tau_c^M$  and  $\tau_c^e$  are plotted for a single day at the SGP Central Facility. Clearly, the empirical algorithm is highly correlated with the Min-derived optical thickness.

Table 1 shows the medians of the distributions of  $\tau_c^M$  and  $\tau_c^e$  over the year 2000, the percent error between these medians, and the mean deviation between  $\tau_c^M$  and  $\tau_c^e$ , for the four sites used in the fit leading to Eq. 4 (indicated by the color-coding in Figure 1). These statistics are also shown for a site, E16, which was *not* part of the fitting process.

The medians differ by less than 10% and there is no obvious bias in the difference, which might indicate a systematic error. The mean deviations seem large, and this could be due to a number of factors, including time registration differences between the MFRSR and broadband instruments, and calibration drifts in the instruments.

A depiction of the distributions of cloud optical thickness, obtained from the two techniques, is shown in Figure 3. These distributions represent the segregation of optical thickness into bins that are one unit wide, and the ordinate of the plot indicates the number of counts per bin. We use site E16—a site not used in our fitting process—and data is shown for the year 2000. The Min-derived and empirical methods are plotted by the blue and red curves, respectively. This figure reveals that the empirical method is able to closely follow the important features of the distribution of  $\tau_c^M$ , including the long tail that extends up to an optical thickness of 200.



**Figure 2.** Time series of Min-derived optical thickness (blue curve), and the optical thickness obtained from the empirical equation (red curve).

**Table 1.** Statistics comparing cloud optical thickness derived from the empirical method and the Min algorithm.

Site	Median $\tau_c^M$	Median $\tau_c^e$	Error (%)	Mean Deviation
E13	28.5	27.9	-2.0	8.6
E22	30.8	29.3	-4.9	6.8
Barrow	14.1	15.3	8.5	2.5
Manus	27.3	27.8	1.8	8.4
E16	32.8	30.6	-6.7	6.9

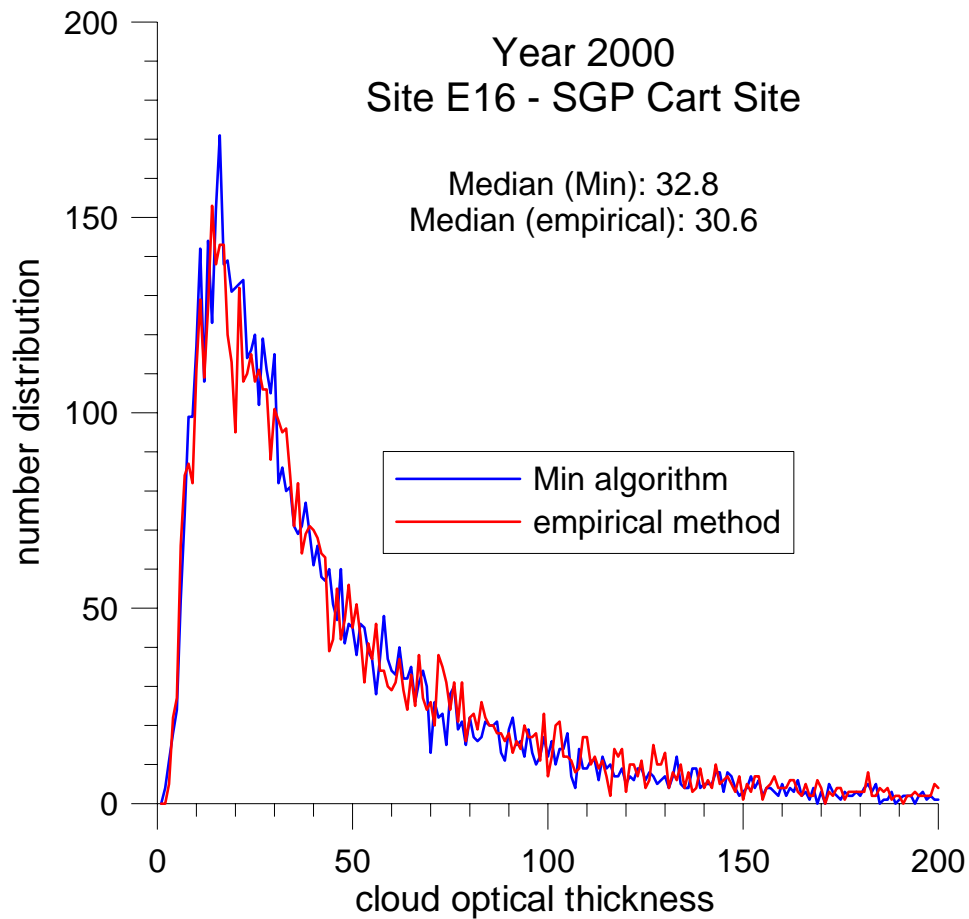


**Figure 3.** Count distribution of cloud optical thickness. The optical thicknesses have been placed in bins that are one unit wide. The blue and red curves have been obtained by binning  $\tau_c^M$  and  $\tau_c^e$ , respectively.

Finally, it is illuminating to apply our empirical method to data obtained from an MFRSR that is completely independent of the ARM system. For this test, the 500-nm channel of the MFRSR provided the spectral irradiance necessary to find  $\tau_c^M$ , while the ‘open’ Silicon detector—a measure of the broadband irradiance—was used to find  $\tau_c^e$ . The MFRSR was deployed in June 2001 in Phoenix, Arizona, as part of a U.S. Department of Energy’s Atmospheric Chemistry Program field study. During this time of year, the skies are nearly cloud free, but for one day, June 25, 2001, clouds were present for part of the day. This provided a small amount of data (98 5-min samples) with which to assess our empirical technique. The surface was assumed to be desert with an albedo of 0.25, taken from Table C-7 in Stull (1991).

Figure 4 shows time series of cloud optical depths obtained from the Min algorithm (blue symbols) and the empirical method (red symbols). We again see that the empirical method is well correlated with the Min optical thicknesses, and can clearly distinguish between low and high optical thickness. For this

day, the mean values of the optical depths are 55 and 50, for the Min and empirical methods, respectively, and the median values are 35 and 29, respectively. The median values exhibit an admittedly large percentage difference, but the small sample size along with the large variation of optical thickness makes the comparison of medians tenuous.

Additionally, some of the difference observed in Figure 4 could be attributed to the differences between the wavelength response of the MFRSR's Silicon detector, which does not detect radiation beyond about  $1\ \mu\text{m}$ , and the broadband radiometers, which sense radiation far past this limit.

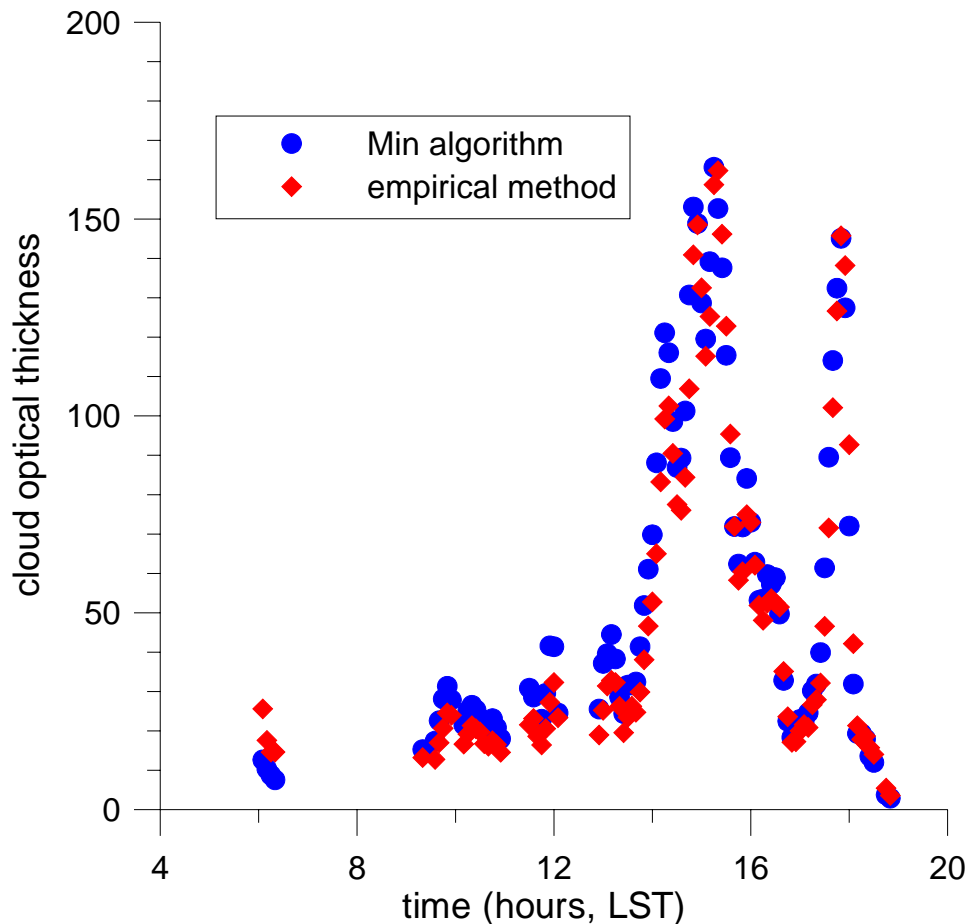


**Figure 4.** Time series of cloud optical thickness for June 25, 2001, from measurements taken at Phoenix, Arizona.

## Caveats

When using the empirical technique described here, it is important to be cognizant of the following caveats:

- We do not know how well this method works for high albedo surfaces, such as snow. We therefore recommend at present that this method only be applied for surface albedos less than 0.30. If the albedo is not known, we recommend assuming a value of 0.15.
- The method is only applicable to fully overcast skies with cloud fractions greater than 0.99. The cloud fraction can be determined using the algorithm of Long (2001).
- This method is not designed for low solar elevation angles,  $\mu < 0.15$ .

## Conclusions

Many algorithms have been developed to retrieve cloud optical thickness from transmission measurements of solar radiation. Those that use broadband irradiances require large amounts of computer time and therefore they are impractical for routine monitoring of cloud optical thickness. To skirt this limitation, we have developed a simple empirical expression that gives cloud optical thickness as a function of  $\mu$ , the surface albedo, the broadband diffuse irradiance, and the broadband “clear-sky” total irradiance (easily obtained from the Long algorithm [2001]).

Cloud optical thicknesses were calculated using the Min and empirical methods for several geographically diverse sites, for data in the ARM system covering the year 2000. For these sites, the medians of the empirical and Min-derived distributions of cloud optical thickness are within 10% of one another, and the shape of the distributions is very similar. When applied to a day of MFRSR data taken in Phoenix, Arizona, in June 2001, the empirical method clearly shows the ability to track optical thickness obtained from the Min algorithm, and it can clearly discriminate between low and high values of this quantity.

With the above evidence in mind, we conclude that the empirical method described here is a useful tool for estimating cloud optical thickness at diverse sites across the world.

## Acknowledgment

This research was sponsored by the U. S. Department of Energy’s Atmospheric Radiation Measurement Program (ARM) Program under Contract DE-AC06-76RL01830 at Pacific Northwest National Laboratory. Pacific Northwest National Laboratory is operated for the U.S. Department of Energy by Battelle Memorial Institute.

## Corresponding Author

J. C. Barnard, [james.barnard@pnl.gov](mailto:james.barnard@pnl.gov), (509) 372-6145

## References

- Barnard, J. C., J. C. Doran, S. Zhong, and C. N. Long, 2001: A comparison of cloud properties at Barrow and SHEBA during the summer of 1998. *Sixth Conference on Polar Meteorology*, 14 – 18 May, San Diego, California.
- Boers, R., 1997: Simultaneous retrievals of cloud optical depth and droplet concentration from solar irradiance and microwave: Liquid Water Path. *J. Geophys. Res.*, **102**, No. D25, 29,881-29891.
- Dutton, E. G., J. J. Michalsky, T. Stoffel, B. W. Forgan, J. Hickey, D. W. Nelson, T. L. Alberta, and I. Reda, 2001: Measurement of broadband diffuse solar irradiance using current commercial instrumentation and a correction for thermal offset errors. *J. Atmos. Oceanic Technol.*, **18**, 297-314.
- Dong, X., T. P. Ackerman, E. E. Clothiaux, P. Pilewskie, and Y. Han, 1997: Microphysical and radiative properties of boundary layer stratiform clouds deduced from ground-based measurements. *J. Geophys. Res.*, **102**, No. D20, 23,829-23,843.
- Long, C. N., and T. P. Ackerman, 2000: Identification of clear skies from broadband pyranometer measurements and calculation of downwelling shortwave cloud effects. *J. Geophys. Res.*, **105**, No. D12, 15,609-15,626.
- Long, C. N., 2001: The shortwave (SW) clear-sky detection and fitting algorithm: Algorithm Operational Details and Explanations, Atmospheric Radiation Measurement Program Technical Report, ARM TR-004. Available URL: [http://www.arm.gov/docs/documents/tech\\_reports/index.html](http://www.arm.gov/docs/documents/tech_reports/index.html)
- Min, Q. and L. C. Harrison, 1996: Cloud properties derived from surface MFRSR measurements and comparison with GOES results at the ARM SGP site. *Geophys. Res. Lett.*, **23** (13):1641-1644.
- Ricchiuzzi, P., S. Yang, C. Gautier, and D. Sowle, 1998: SBDART: A research and teaching software tool for plane-parallel radiative transfer in the Earth's atmosphere. *Bull. Am. Meteorol. Soc.*, **79** (10), 2101-2114.
- Stull, R., 1991: An Introduction to Boundary Layer Meteorology, Kluwer academic Publishers, Dordrecht, The Netherlands.